

UC Davis

UC Davis Previously Published Works

Title

Transcriptional profiling differences for articular cartilage and repair tissue in equine joint surface lesions.

Permalink

<https://escholarship.org/uc/item/0rw2w6z8>

Journal

BMC medical genomics, 2(1)

ISSN

1755-8794

Authors

Mienaltowski, Michael J
Huang, Liping
Frisbie, David D
et al.

Publication Date

2009-09-01

DOI

10.1186/1755-8794-2-60

Peer reviewed

Research article

Open Access

Transcriptional profiling differences for articular cartilage and repair tissue in equine joint surface lesions

Michael J Mienaltowski*^{1,4}, Liping Huang², David D Frisbie³,
C Wayne McIlwraith³, Arnold J Stromberg², Arne C Bathke² and
James N MacLeod¹

Address: ¹University of Kentucky, Department of Veterinary Science, Maxwell H. Gluck Equine Research Center, Lexington, KY, 40546-0099, USA, ²University of Kentucky, Department of Statistics, 817 Patterson Office Tower, Lexington, KY, 40506-0027, USA, ³Colorado State University, College of Veterinary Medicine, Gail Holmes Equine Orthopaedic Research Center, Ft. Collins, CO, 80523-1678, USA and ⁴University of South Florida, College of Medicine, Department of Orthopaedics & Sports Medicine, 12901 Bruce B. Downs Blvd, MDC Box 11, Tampa, FL, 33612, USA

Email: Michael J Mienaltowski* - mmienalt@health.usf.edu; Liping Huang - Liping.Huang@uky.edu;
David D Frisbie - David.Frisbie@ColoState.edu; C Wayne McIlwraith - Wayne.McIlwraith@ColoState.edu;
Arnold J Stromberg - stromberg@uky.edu; Arne C Bathke - arne@uky.edu; James N MacLeod - jnmacleod@uky.edu

* Corresponding author

Published: 14 September 2009

Received: 28 April 2009

BMC Medical Genomics 2009, 2:60 doi:10.1186/1755-8794-2-60

Accepted: 14 September 2009

This article is available from: <http://www.biomedcentral.com/1755-8794/2/60>

© 2009 Mienaltowski et al; licensee BioMed Central Ltd.

This is an Open Access article distributed under the terms of the Creative Commons Attribution License (<http://creativecommons.org/licenses/by/2.0>), which permits unrestricted use, distribution, and reproduction in any medium, provided the original work is properly cited.

Abstract

Background: Full-thickness articular cartilage lesions that reach to the subchondral bone yet are restricted to the chondral compartment usually fill with a fibrocartilage-like repair tissue which is structurally and biomechanically compromised relative to normal articular cartilage. The objective of this study was to evaluate transcriptional differences between chondrocytes of normal articular cartilage and repair tissue cells four months post-microfracture.

Methods: Bilateral one-cm² full-thickness defects were made in the articular surface of both distal femurs of four adult horses followed by subchondral microfracture. Four months postoperatively, repair tissue from the lesion site and grossly normal articular cartilage from within the same femorotibial joint were collected. Total RNA was isolated from the tissue samples, linearly amplified, and applied to a 9,413-probe set equine-specific cDNA microarray. Eight paired comparisons matched by limb and horse were made with a dye-swap experimental design with validation by histological analyses and quantitative real-time polymerase chain reaction (RT-qPCR).

Results: Statistical analyses revealed 3,327 (35.3%) differentially expressed probe sets. Expression of biomarkers typically associated with normal articular cartilage and fibrocartilage repair tissue corroborate earlier studies. Other changes in gene expression previously unassociated with cartilage repair were also revealed and validated by RT-qPCR.

Conclusion: The magnitude of divergence in transcriptional profiles between normal chondrocytes and the cells that populate repair tissue reveal substantial functional differences between these two cell populations. At the four-month postoperative time point, the relative deficiency within repair tissue of gene transcripts which typically define articular cartilage indicate that while cells occupying the lesion might be of mesenchymal origin, they have not recapitulated differentiation to the chondrogenic phenotype of normal articular chondrocytes.

Background

Full-thickness articular cartilage defects that penetrate into the subchondral bone undergo a repair process characterized by the in-growth of fibrous tissue within the lesion [1,2]. Initially, blood from the bone marrow below the articular cartilage fills the defect and forms a fibrin clot [2,3]. Subsequent to vascularization of the defect is the proliferation of granulation tissue over the first 10 days as the clot scleroses [2,3]. The granulation tissue is rich in type I collagen fibers and the cells within the tissue have been traced to a mesenchymal origin [2,4-6]. Within full-thickness defects generated by arthrotomy and controlled drilling into the subchondral bone, not more than 30% of total collagen content is type II four months after surgery [4]. Type I fibrillar collagen predominates the extracellular matrix in repair tissue of most full-thickness defects without graft or transplant [4,7]. Decreases in proteoglycan content also occur which render the repair tissue more rigid and unable to fully protect the joint from biomechanical stress [1,4,5,7]. In addition, morphological differences exist between the cells in repair tissue and the chondrocytes of skeletally mature articular cartilage [3]. Repair tissue anchors incompletely to the surrounding articular cartilage matrix adjacent to the lesion [2]. While repair tissue seems to be primarily derived from stromal cells of mesenchymal origin, the functional similarity of these cells to articular chondrocytes is not completely described. Repair tissue is often called fibrocartilage or hyaline-like repair cartilage, though it does not necessarily contain an actual chondrocyte cell population.

The engineering of repair tissue cells is widely investigated in an attempt to improve the chondral surface within injured joints. Techniques like microfracture have been developed in an effort to facilitate healing of the articular surface with cells from the subchondral bone [6,8-13]. There is also a focus on manipulating repair tissue, implanted stem cells, and even autologous chondrocyte transplants in an effort to generate more hyaline-like phenotypes [14,15]. Assessment of the similarity of repair tissue to cartilage is typically done by monitoring established matrix biomarkers, such as type I collagen, type II collagen, and aggrecan core protein. Even with the introduction of growth factors or scaffolds of maintenance proteins associated with the chondrocyte phenotype, the repair tissue is still unable to completely restore the structural and biomechanical integrity of the joint surface, consistent with the limited capacity of articular cartilage to heal.

In this study, we used an equine cDNA microarray containing 9,413 probe sets to compare gene expression profiles of grossly normal articular cartilage and repair tissue occupying medial femoral condyle full-thickness defects in the femorotibial joints of skeletally mature horses four

months after a microfracture surgical procedure. The hypothesis tested was that the cells occupying repair tissue four months postoperatively are not identical to articular chondrocytes. Consequently, we would expect the transcriptomes of cells from each tissue to have substantial differences, especially with respect to the expression of cartilage matrix biomarkers.

Methods

Animals

Articular cartilage defects were made in the axial weight-bearing portion of the medial femoral condyles of four adult Quarterhorses (2-3 years) as previously described by Frisbie *et al.* [6,16] within the guidelines set forth in an Institutional Animal Care and Use Committee-approved protocol at Colorado State University. Briefly, one-cm² full-thickness articular cartilage lesions were arthroscopically made bilaterally which included the removal of the calcified cartilage layer. This was followed by microfracture penetration of the subchondral bone to create perforations with an approximate spacing of 2-3 mm and depth of 3 mm uniformly within the defect site. The horses were maintained for four months in box stalls (3.65 m × 3.65 m) with controlled hand walking. After euthanasia, repair tissue from the lesions and full-thickness grossly normal articular cartilage from within the same joint were collected from each stifle, rinsed in sterile phosphate-buffered saline, snap-frozen in liquid nitrogen, and stored at -80°C.

Histology

Samples were also collected and prepared for histological analyses as described in Frisbie *et al.* [17]. Briefly, repair tissue and adjacent cartilage were trimmed with a standard bone saw and Exakt bone saw with a diamond chip blade (Exakt Technologies, Oklahoma City, OK, USA), placed into histological cassettes, and then fixed in 10% neutral buffered formalin for a minimum of 2 days. Samples were then applied to 0.1% EDTA/3%HCl decalcification solution (Thermo Scientific Richard-Allan Decalcifying Solution, cat. no. 8340) which was replenished every three days until specimens were decalcified. Specimens were embedded in paraffin and sectioned at 5 µm. Sections were stained with hematoxylin and eosin or with Safranin-O.

Total RNA Isolation and Linear Amplification

Normal articular cartilage was reduced to powder with a BioPulverizer (BioSpec Products, Bartlesville, OK, USA) under liquid nitrogen and total RNA was isolated as described by MacLeod *et al.* [18,19]. Briefly, total RNA was isolated in a buffer of 4 M guanidinium isothiocyanate, 0.1 M Tris-HCl, 25 mM EDTA (pH 7.5) with 1% (v/v) 2-mercaptoethanol, followed by differential alcohol and salt precipitations and then final purification using QIA-

GEN RNeasy columns [18-21]. Repair tissue sample sizes were minimal in size (10-50 mg). Repair tissue was placed in QIAzol reagent (QIAGEN), cut into 1-mm³ slices, and total RNA isolated using the QIAGEN RNeasy Lipid Tissue Mini Kit. RNA quantification and quality assessments were performed with a NanoDrop ND-1000 and a BioAnalyzer 2100 (Agilent, Eukaryotic Total RNA Nano Series II). Total RNA (1 µg) from each tissue sample received one round of linear amplification primed with oligo-dT (Invitrogen - SuperScript RNA Amplification System) [22,23]. Two micrograms of amplified RNA were then used as a template to create fluorescent dye-coupled single-stranded aminoallyl-cDNA probes (Invitrogen - SuperScript Indirect cDNA Labeling System, Molecular Probes - Alexa Fluor 555 and 647 Reactive Dyes). For each sample, probes were coupled to both Alexa Fluor dyes individually so that a dye swap comparison could be made.

Transcriptional Profiling

Microarray slides were printed with clones selected from a cDNA library generated using equine articular cartilage mRNA from a 15-month old Thoroughbred [24]. Microarray slides were pre-hybridized in 20% formamide, 5× Denhardt's, 6× SSC, 0.1% SDS, and 25 µg/ml tRNA for 45 minutes. The slides were then washed five times in deionized water, once in isopropanol, and spun dry at 700 g for 3 minutes [25]. Two labeled cDNA samples, one repair tissue and the other normal cartilage from the same joint, were combined with 1× hybridization buffer (Ambion, 1× Slide Hybridization Buffer #1, cat. no. 8801), incubated for 2 minutes at 95°C, and then applied to the slide under a glass lifterslip for 48 hours at 42°C. All hybridizations were performed in duplicate with a dye swap to eliminate possible dye bias [26]. Sequential post-hybridization washes were each for 5 minutes as follows: 1× SSC, 0.2% SDS at 42°C; 0.1× SSC, 0.2% SDS at room temperature; and twice with 0.1× SSC at room temperature. The slides were then spun dry under argon gas at 700 g for 3 minutes. Each slide was coated once in DyeSaver 2 (Genisphere) and allowed to dry for 10 minutes. Slides were scanned using a GenePix 4100A scanner and spot intensities were computed using GENEPIX 6.0 image analysis software (Axon Instruments/Molecular Devices).

Statistics and Analysis

Raw mean intensity data for each probe set pair of all the microarray scans were statistically analyzed by planned linear contrast [27] using SAS (SAS Institute, Cary, NC). One sample t-tests were performed, which were followed by a Benjamini-Hochberg correction based on a false discovery rate of 2.2% for probe sets with a p-value < 0.01 [28]. Differences in the transcriptional profiling data between repair tissue and articular cartilage were analyzed based on a linear model formulation with fixed tissue and dye effect, and random chip, horse, and leg effect. A dye swap design was used, so for each available leg, the sum

of the two measurements corresponding to the articular cartilage was subtracted from the sum of the measurements corresponding to the repair tissue. Each intensity measurement (*I*) is modeled statistically as:

$$I = d + c + t + h + l + E$$

with the components designated as follows: *d*, additive effects due to dye (red or green); *c*, chip effect (1-16); *t*, tissue (repair or normal); *h*, horse (1-4); *l*, leg (left or right); *E*, statistical error. The dye swap design yields two outcomes per location and tissue type. Thus, for each of the eight locations corresponding to a particular leg of a particular horse, a new aggregated quantity is calculated that takes into account all measurements related to this location. The only remaining systematic effect represents the expressional difference between tissues with remaining statistical error. Since there were 4 horses with 2 femorotibial joints per horse, eight such tissue differences were evaluated. Gene identity was assigned for each microarray ID from an internal annotation database through selection of either the best RNA RefSeq BLAST ($E < 1 \times 10^{-7}$) or Protein RefSeq BLAST ($E < 1 \times 10^{-5}$) result [29-31]. Gene ontology (GO) annotation was derived from batch queries of the Database for Annotation, Visualization, and Integrated Discovery (DAVID) Bioinformatics tool or manually through individual NCBI Entrez Gene queries [32,33]. The human ortholog of each gene was predicted and used for the determination of overrepresentation of GO categories via Expression Analysis Systemic Explorer (EASE) standalone software [32,34]. Statistical data, fold change quantities, and GO annotations were managed within an Excel spreadsheet (Microsoft, Redmond, WA). Microarray data are available at the NCBI Gene Expression Omnibus (GEO) under Series Accession GSE11760.

Validation of Microarray Hybridization Results with RT-qPCR

Differential expression for selected genes was validated using quantitative polymerase chain reactions (RT-qPCR). Briefly, total RNA was reverse-transcribed into cDNA using an oligo-dT primer with the Promega Reverse Transcription System (Promega, cat. no. A3500). Quantitative "real-time" PCR (7500 Sequence Detection and 7900 HT Fast Real-Time PCR Systems, Applied Biosystems, Foster City, CA) was performed using TaqMan Gene Expression Master Mix (Applied Biosystems) and intron-spanning primer/probe sets (Assays-by-Design, Applied Biosystems) designed from equine genomic sequence data (Ensembl - http://www.ensembl.org/Equus_caballus/index.html; UCSC Genome Browser - <http://genome.ucsc.edu>). Beta-2-microglobulin (B2M) and large ribosomal protein P0 (RPLP0) were selected as endogenous control transcripts because they showed the greatest stability for the sample set as defined by the geNorm reference gene application (data not shown) [35]. Steady

state levels of mRNA encoding type I procollagen (COL1A2), type II procollagen (COL2A1), cartilage oligomeric matrix protein (COMP), dermatopontin (DPT), fibroblast activation protein (FAP), and tenascin-C (TNC) were selected for validation (Table 1). Amplification efficiencies were measured by the default fit option of Lin-RegPCR while maintaining the cycle threshold as a data point within the measured regression line [36]. Since amplification efficiencies for some of the genes were determined to be different between sample groups (normal and repair) by paired t-test, mean group efficiencies were utilized for adjustment of results for each gene (data not shown) [37]. Relative expression levels of target genes were normalized to the relative quantities of endogenous control genes using geometric averaging with the geNorm VBA applet [35]. For each gene of interest, mean fold change was determined by first finding the difference in transcript abundance between normal and repair samples from each leg and then by determining the mean difference amongst all legs for that gene. Statistical analysis of RT-qPCR results was performed with a general linear model (GLM) strategy using SPSS software with consideration for variables of horse, leg, and tissue. One-tail ($\alpha = 0.05$) test of the hypothesis that microarray data are valid was considered for tissue effect, which is the significance reported. By the same GLM analyses, no significant "within horse" leg effect was demonstrated for any of the genes validated (data not shown).

Results

Repair tissue histology

Tissue samples were harvested four months after surgical induction of full-thickness cartilage lesion with microfracture. Gross examination revealed repair tissue within each lesion that was dimpled in appearance and not completely level with the articular surface (Figure 1A, D). His-

tologically, repair tissue generally had homogeneous matrix architecture with elongated, flattened cells (Figure 1G) that interfaced with surrounding articular cartilage (Figure 1H). Varying levels of repair tissue were noted with some lesions having a poor response (Figure 1A-C), while others appeared to respond better (Figure 1D-F). Safranin-O staining demonstrated that the repair tissue was generally proteoglycan-deficient relative to the adjacent normal articular cartilage surrounding the lesions (Figure 1C), but there was variation with some repair tissue samples showing evidence of proteoglycan content (Figure 1F).

Overall level of differential gene expression

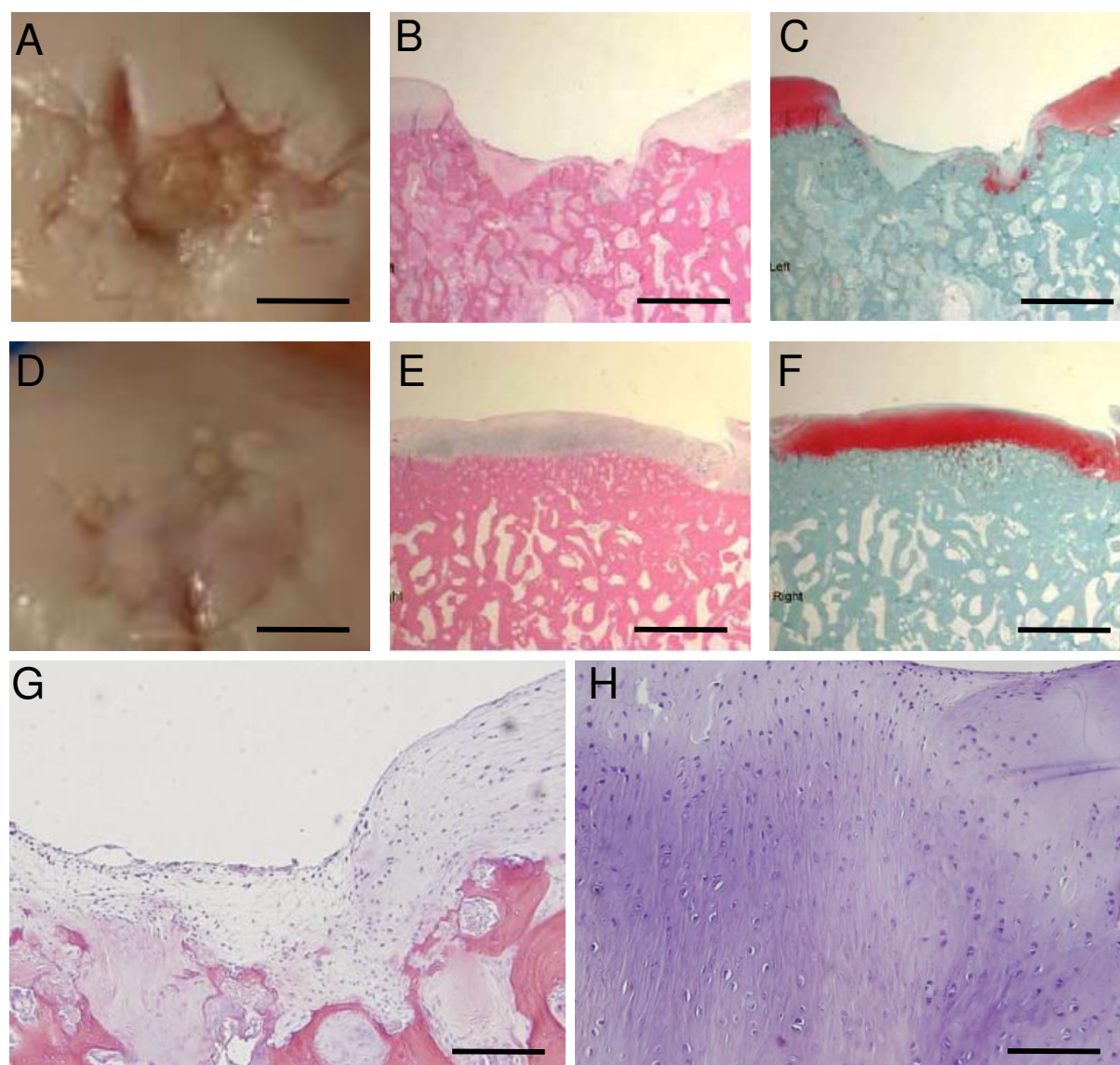
A total of 4,269 probe sets (45.4%) were differentially expressed ($p < 0.01$; Figure 2A). A clear transcriptome divergence was evident between the two tissue types (Figure 2B). After Benjamini-Hochberg correction, 3,327 (35.3%) significant probe sets remained (Figure 3). Of these probe sets, 1,454 demonstrated greater transcript abundance in repair tissue relative to grossly normal articular cartilage, and 1,873 demonstrated greater transcript abundance in normal articular cartilage relative to repair tissue. Assessment of probe set annotation produced 2,688 significant probe sets with known gene identities. Correcting for redundancy where different probe sets hybridize to the same mRNA transcript yielded 2,101 unique gene symbols. Of these, 858 gene symbols were present at higher steady-state levels in repair tissue and are designated *repair > normal*, while 1,243 of the gene symbols are designated *normal > repair* (Figure 3).

Ontological differences

When significant probes are organized according to molecular function ontology with a fold change threshold of two, ontological categories of differentially abundant

Table 1: Primer nucleotide sequences used in RT-qPCR assays for genes described in the study.

Gene Name	Gene Symbol	Forward Primer	Reverse Primer
Beta-2-microglobulin	B2M	5-CGGGCTACTCTCCCTGACT-3	5-GTGACGTGAGTAAACCTGAACCTT-3
Ribosomal protein, large, P0	RPLP0	5-CTGATTACACCTTCCCACTTGCT-3	5-AGCCACAAATGCAGATGGATCA-3
Procollagen, type I, alpha 2	COL1A2	5-TGAGACTTAGCCACCCAGAGT-3	5-GCATCCATAGTGCATCCTTGATTAGG-3
Procollagen, type II, alpha 1	COL2A1	5-CTGGCTTCAAAGGCGAACAAG-3	5-GCACCTCTTTTGCCTTCTTCAC-3
Cartilage oligomeric matrix protein	COMP	5-CGAGCCCGGCATCCA-3	5-CCCAGGGCCTGTGGAG-3
Dermatopontin	DPT	5-GGAGATCAACAGGGCTGGAAT-3	5-CCGCCACCAGTCCATTGTT-3
Fibroblast activation protein	FAP	5-AGACTATCTTCTCATCCACGGAACA-3	5-CCGGATATGCCGTGGTTCTG-3
Tenascin-C	TNC	5-TCAGCCATCACTACCAAGTTCAC-3	5-GAACCTCAGTAGCAGTCAAATCTCT-3

**Figure 1**

Gross and histological assessment of repair tissue. At the four month post-operative time point, gross assessment of the repair tissue indicated variations in the healing response (A, D). Moreover, the repair tissue was not fully congruent with the surrounding articular cartilage within each lesion (B, E). Histologically, variations in the repair resulted in elongated and flattened cells as observed with H&E staining (G, 10 \times) surrounded by variable levels of proteoglycan-deficient matrix as assessed by Safranin-O staining (C, F). The interface between repair tissue and surrounding cartilage is evident (H, 20 \times). Representative lesions depicted are from Horse 4 (Left: A, B, C, G; Right: D, E, F, H). Scale bar: 5 mm in A, D; 2.50 mm in B, C, E, F; 250 microns in G; 125 microns in H.

transcripts emerge by EASE analyses (Tables 2 and 3). Categories statistically overrepresented in normal articular cartilage include skeletal development and glycosaminoglycan binding, which contain many of the conventional cartilage biomarkers (Table 2). Protease and endopeptidase inhibitor activities were also overrepresented for normal cartilage; these categories contain matrix metalloproteinase inhibitors essential to the main-

tenance of cartilage matrix (Table 2). In contrast, the categories statistically overrepresented in repair tissue (immune response, cytoskeletal and cell component organization, and histogenesis) are indicative of wound healing or tissue re-modeling (Table 3). One shared overrepresented category is calcium ion binding, which is involved with protein-folding conformation of matrix molecules and chondrocyte differentiation, among other

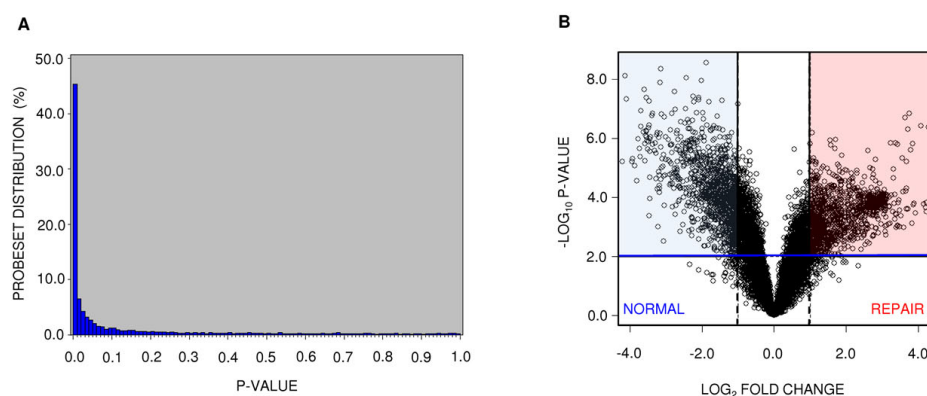


Figure 2

Microarray profiling data distributions. The distribution of p-values for differential gene expression comparing articular cartilage to repair tissue using 8 replicates (4 left legs and 4 right legs from 4 horses) is demonstrated in a histogram (A); the column at the far left are those differentially expressed at $p < 0.01$ and represents 4269 probe sets, or 45.6% of the microarray. (B) A volcano plot illustrates the divergent distribution of probe sets between normal articular cartilage and repair tissue. \log_2 -fold change differences of transcript abundance are represented across the horizontal axis; fold changes greater than 2-fold are located outside of the vertical dotted lines. Significance ($-\log_{10}$ p-value) is represented on the y-axis with $p < 0.01$ located above the blue horizontal line. Probe sets within the blue shaded region have a fold change ≥ 2 at $p < 0.01$ in normal articular cartilage relative to repair tissue. Probe sets within red shaded region have a fold change ≥ 2 at $p < 0.01$ in repair tissue relative to normal articular cartilage.

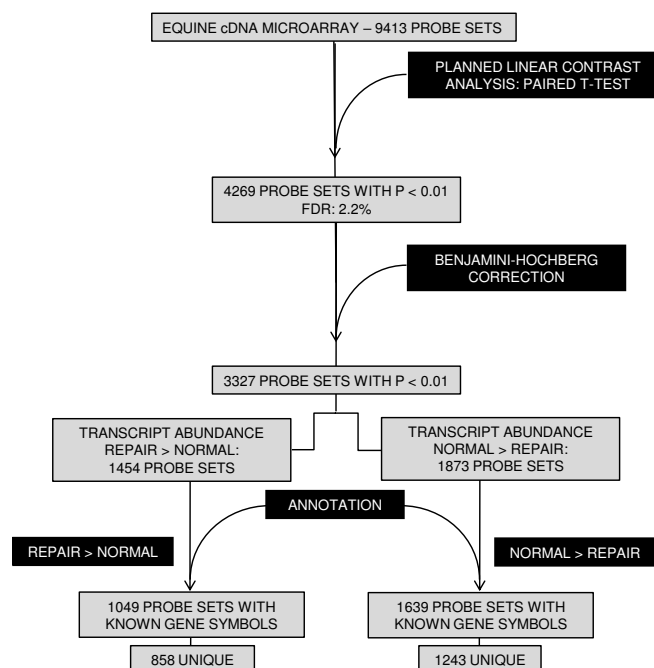


Figure 3

Flowchart of cDNA microarray data analysis. Expression data were initially analyzed by planned linear contrast with a Benjamini-Hochberg correction yielding 35.3% of the probe sets on the microarray demonstrating significant differential gene expression ($p < 0.01$). Of these, 43.7% and 56.3% of the probe sets represented increased relative transcript abundance for repair tissue > normal cartilage and normal cartilage > repair tissue, respectively. When annotation is applied to these probe sets, 2688 (80.8%) have known gene symbols with a redundancy across this subset of probe sets equal to 21.8% yielding 2101 unique gene symbols.

Table 2: Overrepresented ontological categories for transcripts with >2-fold difference in normal articular cartilage versus repair tissue.

GO System	Gene Category	List Hits	List Total	Population Hits	Population Total	EASE Score
Cellular Component	extracellular	69	380	244	2556	2.01E-08
Biological Process	skeletal development	21	379	55	2575	0.00005
Molecular Function	receptor activity	53	385	218	2611	0.00012
Cellular Component	extracellular matrix	30	380	100	2556	0.00015
Biological Process	development	82	379	394	2575	0.00036
Molecular Function	signal transducer activity	81	385	393	2611	0.00059
Molecular Function	calcium ion binding	34	385	134	2611	0.00129
Biological Process	regulation of transcription (3)	82	379	410	2575	0.00134
Molecular Function	glycosaminoglycan binding	12	385	31	2611	0.00318
Molecular Function	endopeptidase inhibitor activity (2)	11	385	27	2611	0.00341
Molecular Function	protease inhibitor activity	11	385	27	2611	0.00341
Cellular Component	membrane (2)	148	380	842	2556	0.00553
Molecular Function	steroid hormone receptor activity	7	385	13	2611	0.00668
Biological Process	transcription	83	379	441	2575	0.00764
Molecular Function	insulin-like growth factor binding	6	385	10	2611	0.00893

Redundant or similar categories were removed. When present, the number of redundant or similar categories are indicated in parentheses within the listed "gene category." "GO System" represents the major gene ontological system (i.e., cellular component, biological process, or molecular function). "Gene category" shows a descriptive term shared by a group of genes. "List hits" are the numbers of differentially abundant transcripts that belong to the gene category. "List total" is the number of differentially expressed genes within the corresponding cellular component, biological process, or molecular function system. "Population hits" represent the total number of genes found on the microarray possessing that specific gene category annotation (e.g., extracellular, skeletal development, etc.). "Population Total" represents the total number of genes found on the microarray possessing that ontological system annotation. "EASE score" is a measure of overrepresentation that scales the results of a statistical analysis (Fisher's exact test) by biasing against categories supported by few genes.

functions. A second overrepresented category common to the two tissue types was extracellular matrix component. This result is quite plausible since extracellular matrix (ECM) plays an essential role in defining the phenotypes of both tissues. Functional differences are demonstrated by individual transcript abundance for ECM components involved in processes such as fibrillogenesis and proteoglycan synthesis which are further delineated below.

Individual genes

Expression differences for genes encoding biomarkers typically associated with normal articular cartilage and repair tissue corroborate previous reported findings (Figure 4). That is, transcript abundance for collagen types II and IX were greater in normal articular cartilage relative to repair tissue. The expression of type I collagen and several type-I-associated collagen types (V, VI, XII, XV) were up-regu-

lated in repair tissue relative to normal articular cartilage. Moreover, transcript abundance was greater in normal cartilage for proteoglycans, an associated sulfotransferase, non-collagenous adhesion proteins, and skeletal development biomarkers linked to cartilage development. In contrast, transcripts were up-regulated in repair tissue for Tenascin- C and matrix metalloproteinase 3, which are both associated with wound healing.

Other genes with limited or no established functional annotation in chondrocytes were also differentially expressed between normal articular cartilage and repair tissue. Within the angiogenesis category, transcripts encoding vascular endothelial growth factor and the serpin peptidase inhibitor SERPINE1 had higher steady state levels in repair tissue (Figure 5). Also represented were genes involved in cell adhesion, cell communication, skel-

Table 3: Overrepresented ontological categories for transcripts with >2-fold difference in repair tissue versus normal articular cartilage.

GO System	Gene Category	List Hits	List Total	Population Hits	Population Total	EASE Score
Biological Process	immune response	23	270	98	2575	0.00032
Biological Process	defense response	23	270	103	2575	0.00066
Cellular Component	cytoskeleton	39	275	216	2556	0.00095
Cellular Component	actin cytoskeleton	18	275	73	2556	0.00133
Biological Process	response to biotic stimulus	26	270	130	2575	0.00148
Biological Process	organelle organization and biogenesis	21	270	96	2575	0.00162
Biological Process	cytoskeleton organization and biogenesis	16	270	65	2575	0.00216
Cellular Component	extracellular matrix	21	275	100	2556	0.00368
Biological Process	histogenesis	7	270	16	2575	0.00398
Biological Process	cell motility	18	270	84	2575	0.00492
Biological Process	response to external stimulus	36	270	220	2575	0.00569
Molecular Function	calcium ion binding	25	279	134	2611	0.00627
Biological Process	protein complex assembly	10	270	34	2575	0.00646
Biological Process	cell adhesion (3)	26	270	145	2575	0.00685
Molecular Function	hydrogen ion transporter activity (2)	13	279	53	2611	0.00808

Redundant or similar categories were removed. When present, the number of redundant or similar categories are indicated in parentheses within the listed "gene category." "GO System" represents the major gene ontological system (i.e., cellular component, biological process, or molecular function). "Gene category" shows a descriptive term shared by a group of genes. "List hits" are the numbers of differentially abundant transcripts that belong to the gene category. "List total" is the number of differentially expressed genes within the corresponding cellular component, biological process, or molecular function system. "Population hits" represent the total number of genes found on the microarray possessing that specific gene category annotation (e.g., extracellular, skeletal development, etc.). "Population Total" represents the total number of genes found on the microarray possessing that ontological system annotation. "EASE score" is a measure of overrepresentation that scales the results of a statistical analysis (Fisher's exact test) by biasing against categories supported by few genes.

etal development, and carbohydrate and proteoglycan metabolism. Of note was increased transcript abundance in repair tissue for proliferative cell markers like fibroblast activation protein (FAP) and stathmin-1, as well as the inflammatory mediator cyclooxygenase-2 (COX2) (Figure 5).

Quantitative PCR validation

Steady-state transcript abundance was measured for endogenous controls beta-2-microglobulin (B2M) and large ribosomal protein P0 (RPLP0), as well as target genes type I procollagen alpha-2 chain (COL1A2), type II procollagen alpha 1 chain (COL2A1), cartilage oligomeric matrix protein (COMP), dermatopontin (DPT), fibroblast activation protein (FAP), and tenascin-C (TNC). Relative quantification of target transcripts revealed significant

increases in mRNA abundance for COL2A1 and COMP in normal articular cartilage (Figure 6). Fold change differences were similar or slightly greater than what was measured by microarray profiles. Increased COL1A2, DPT, and FAP transcript abundance for repair tissue was also validated by RT-qPCR (Figure 6). Transcript abundance for TNC in repair tissue demonstrated an increasing trend by RT-qPCR, though significance was not achieved (Figure 6).

Discussion

Histological analyses and transcriptional studies identified clear differences between chondrocytes of grossly normal articular cartilage and the cells present in repair tissue of full-thickness articular lesions following a microfracture surgical procedure. At four months post-surgery,

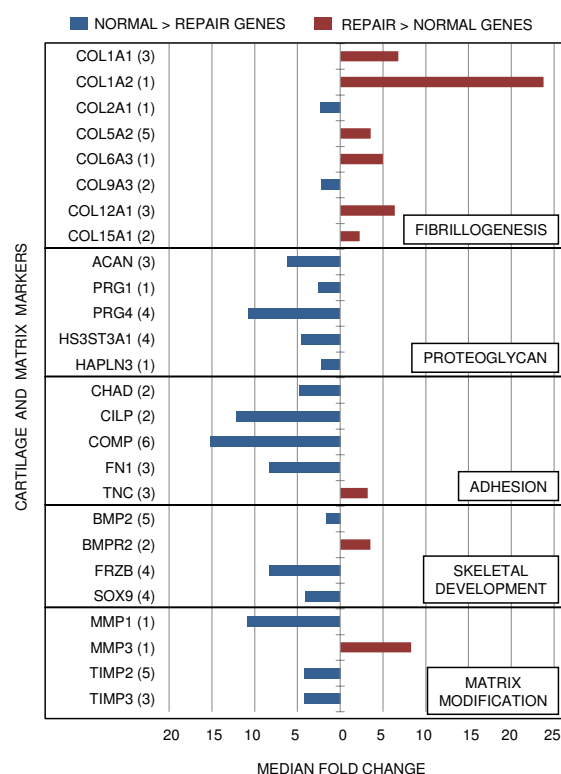


Figure 4
Microarray transcriptional profiles of articular cartilage and repair tissue molecules/biomarkers. Bars represent median fold changes of differentially expressed genes ($p < 0.01$) previously associated with cartilage and fibrocartilage. Gene symbols are organized by functional annotation and are listed with the number of representative probe sets in parentheses.

repair tissue is morphologically discernible from normal cartilage. Type I collagen transcripts are detected in the repair tissue, and much of the repair tissue is proteoglycan-deficient. Moreover, a substantial transcriptional divergence is readily apparent between the two cell types even at a genomic level. Analyses of overrepresented gene categories for differentially expressed transcripts demonstrate broad functional differences.

Conventional biomarker transcripts used to characterize a chondrocytic phenotype indicated that the repair tissues in this sample set were quite different from the adjacent articular cartilage in the same joint. Increased transcript levels for types II and IX collagen were found in the articular cartilage (Figure 4). Quantitative RT-PCR indicated a 16.1-fold expression difference for COL2A1 in articular cartilage relative to repair tissue ($p = 0.0090$, Figure 6B). In contrast, abundance of transcripts associated with type I collagen-rich fibrous tissues were greater in repair tissue

(Figure 4). Steady-state mRNA levels for COL1A2 were 77.1-fold higher in repair tissue relative to articular cartilage ($p = 0.0485$, Figure 6A). These transcriptional data directly support published biochemical results which demonstrated differing collagen type I: type II ratios for articular repair tissue and perilesional articular cartilage through detection of cleaved peptides [4,7]. Differences in the magnitude of fold changes in microarray and RT-qPCR results can be explained by the differences in dynamic range of detection between hybridization-based assays and amplification-based assays [38]. Notable differences for proteoglycans between repair tissue and the surrounding articular cartilage were observed with transcript levels and by Safranin-O staining (Figures 1, 4). Proteoglycan differences have also been noted through Safranin-O staining of articular repair tissue in the distal femur of the New Zealand White rabbit [2] and in the distal radial carpal bone of the horse [7], relative to proteoglycan content of perilesional articular cartilage in both studies.

Divergent characteristics between articular cartilage and repair tissue extend to transcripts of other matrix proteins. Transcripts encoding cartilage macromolecules believed to play a role in cell-cell and cell-matrix interactions were significantly less abundant in repair tissue relative to normal articular cartilage (Figure 4). Such transcripts included chondroadherin (CHAD), cartilage intermediate layer protein (CILP), cartilage oligomeric matrix protein (COMP), and fibronectin (FN1) [39-44]. COMP interacts with type II collagen for fibrillogenesis and has been shown to bind to the chondroitin sulfate glycosaminoglycans associated with aggrecan. COMP expression is initially up-regulated in chondrocytes exposed to increased dynamic compression [45,46], those from the superficial zone in fibrillated OA cartilage [47], and chondrocytes adjacent to an OA lesion [44]; however, transcript levels in repair tissue at the four month time point were 30.5-fold lower ($p = 0.0010$, Figure 6C). Matrix molecules like CILP which are present in normal cartilage slow down the responsiveness of chondrocytes to insulin-like growth factor 1 (IGF-1) as a result of accumulation of calcium pyrophosphate dehydrate [43]. Thus, CILP might inhibit the ability of the surrounding chondrocytes to expand and occupy the lesion [43]. Transcript abundance for hypoxia inducible transcription factor 2 α (HIF-2 α) was up-regulated in normal cartilage (Figure 5) and has been found to support the cartilage phenotype by (SRY-box 9) SOX9 induction of matrix genes [48]. In contrast, tenascin-C (TNC), which is typically found in provisional matrices throughout development and wound healing [49-52], demonstrated greater transcript levels in repair tissue by microarray analyses (Figure 4). While statistical significance was not confirmed by RT-qPCR ($p = 0.0665$, Figure 6F), upregulation of TNC has been noted in early stages of

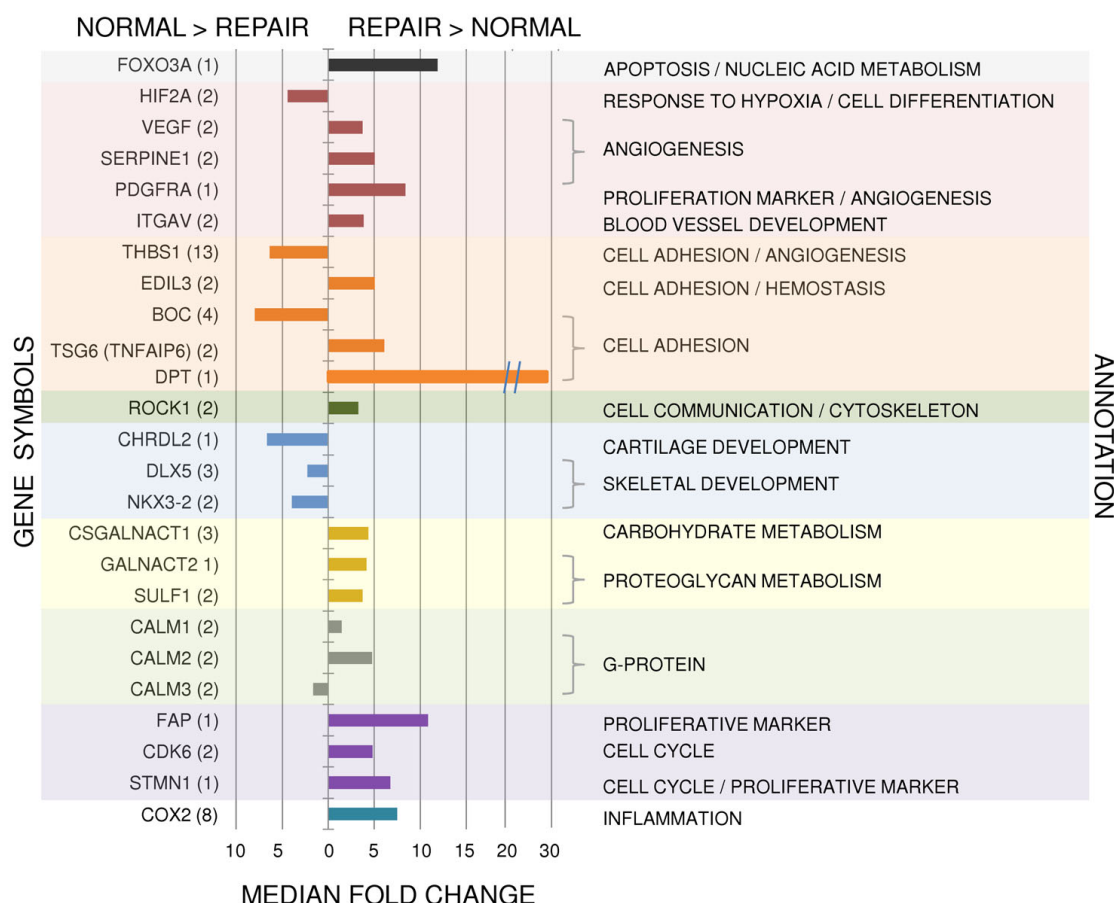


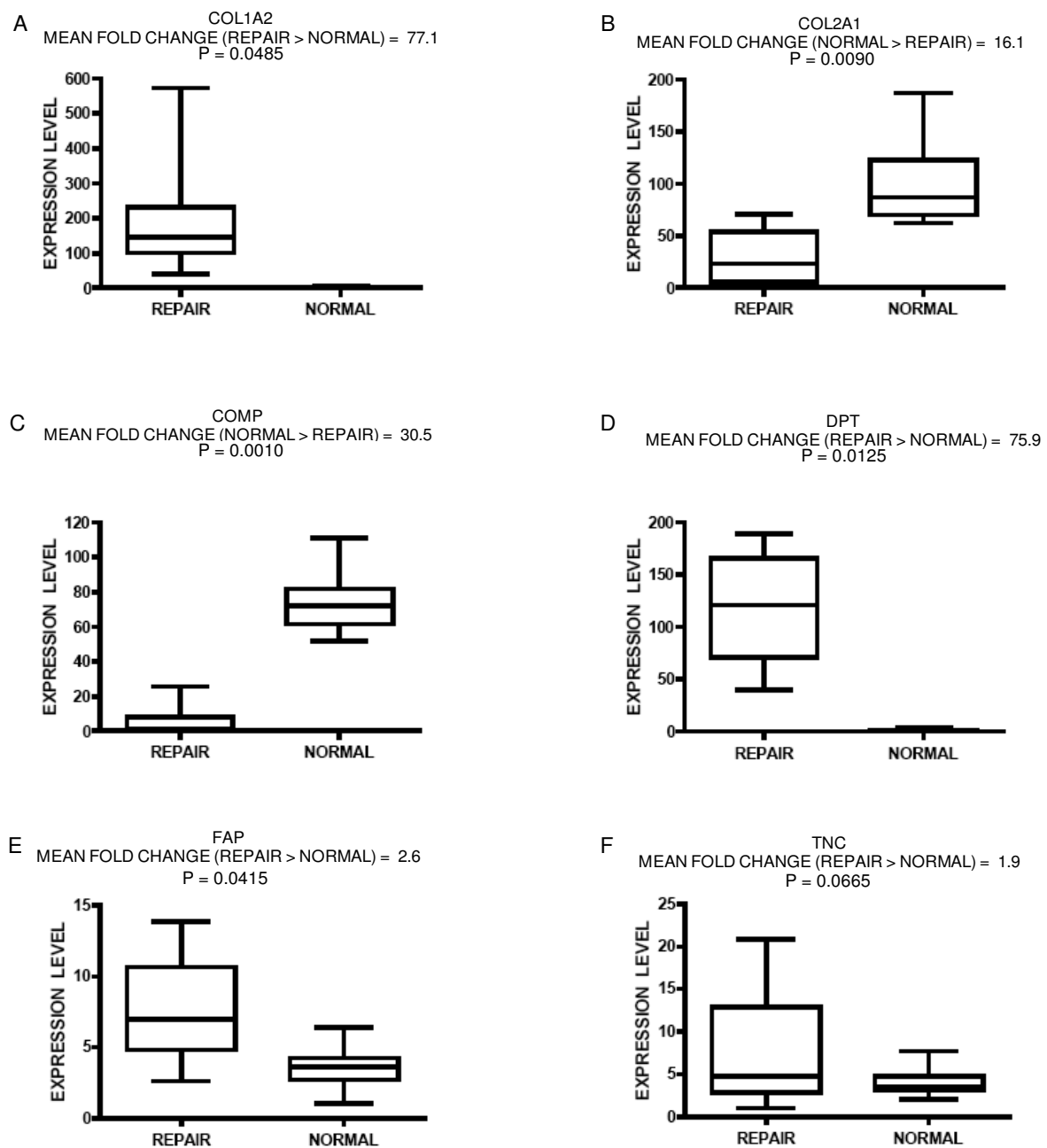
Figure 5

Microarray transcriptional profiles for representative genes of interest. Median fold changes are shown for differentially expressed genes ($p < 0.01$) which further distinguish normal articular cartilage and repair tissue. Individual genes are organized by molecular function. Gene symbols are given with the number of representative probe sets in parentheses.

osteoarthritis and also during the repair process of many other tissues through *in situ* hybridization, immunohistochemistry, and knockout mouse studies [49,53-55]. Based on its function in the expansion of provisional matrices, it is likely that analyses of earlier time points would have detected greater divergence of TNC mRNA levels.

Within the repair tissue, differential expression was noted for transcripts encoding proteins involved in wound healing and matrix synthesis. Shapiro *et al.* have shown that stromal cells of mesenchymal origin from the subchondral bone enter into the wound with the blood which fills the full-thickness lesion [2]. With angiogenic cues such as vascular endothelial growth factor (Figure 5) and vascularization from the subchondral bone, these cells proliferate within the granulation tissue to occupy the lesion [2,56,57]. Increased transcript abundance of fibroblast activation protein (FAP) is consistent with the proliferative cellular response reported by Shapiro *et al.* (Figure 5)

[2]. RT-qPCR indicated a 2.6-fold relative expression difference for FAP in repair tissue four months post-microfracture relative to articular cartilage ($p = 0.0415$, Figure 6E). Assessment of FAP expression at additional time points during the repair process would further delineate its importance. Steady-state levels of dermatopontin (DPT) were also elevated in repair tissue (Figures 5, 6D). Fibrillogenesis of type I collagen is accelerated by DPT, which has previously been localized in skin fibroblasts, skeletal muscle, heart, lung, bone, and chondrocytes that de-differentiate while expanding in monolayer culture [58-60]. DPT interacts synergistically with decorin and transforming growth factor- β 1 to bolster collagen synthesis and accelerate fibrillogenesis to the point of decreasing fibril diameters in proliferating skin fibroblast cultures [59]. A wound healing process is further indicated by the 7.5-fold up-regulation of cyclooxygenase 2 (COX2, Figure 5), an inflammatory modulator shown to be essential in the repair of bone fractures and growth plate lesions [61].

**Figure 6**

RT-qPCR validation of differential gene expression. Significant up-regulation of COL2A1 (B) and COMP (C) gene expression in normal articular cartilage relative to repair tissue was confirmed. Higher steady-state levels of COL1A2 (A), DPT (D), and FAP (E) transcripts in repair tissue were also confirmed. Gene expression of TNC (F) demonstrates a trend of increased steady state abundance in repair tissue relative to normal articular cartilage, though statistical significance was not achieved. Steady state mRNA levels for each gene were standardized to the sample with the lowest value. Plots are depicted as box and whisker plots demonstrating the median (solid line), upper and lower quartiles, and highest and lowest values (range bars). Mean fold differences are given above the box and whisker plots for each gene; one-tailed general linear model ($\alpha = 0.05$) statistical analysis applied with SPSS software.

Transcript profiles for COX2 and S100 protein are compatible with chondrogenic differentiation of stromal cells [61,62], but the consistent deficiency of cartilage matrix protein biomarkers highlighted by the switch of type I collagen (COL1A1, COL1A2) in place of type II collagen (COL2A1) as the primary fibrillar collagen document the failure of true hyaline cartilage restoration.

A limitation of this study must be noted. Tissues utilized in these experiments included repair tissue and grossly normal articular cartilage from within the same joint. Thus, any gene expression differences between grossly normal cartilage within the lesioned joint and cartilage from an intact articular surface from another joint were not assessed. Differences have been reported with intact cartilage from human OA joints [63]. However, equine joints used for the current sample set had minimal OA and the defects were freshly created in the medial femoral condyles four months prior to tissue sample collection.

Conclusion

Transcriptional profiling data support the hypothesis and indicate that repair tissue cells following a microfracture surgical procedure are still very different from normal articular chondrocytes at the four month postoperative time point. The cell and matrix organizational phenotypes of repair tissue are substantially different from those of chondrocytes within mature articular cartilage that has developed and adapted to biomechanical strains from birth. Microarray data in the current study corroborate what has been reported previously at mRNA and protein levels for conventional cartilage biomarkers, but extends our understanding by documenting differences in transcript abundance across multiple ontology categories and genes not previously studied in these tissues. By directing further research toward factors which contribute to the transcriptome dissimilarities of repair tissue and normal articular cartilage phenotypes, we should advance our understanding of the repair process and improve upon therapeutic strategies directed at restoring the structural and biomechanical integrity of the joint surface.

List of Abbreviations

B2M: beta-2-microglobulin; CHAD: chondroadherin; CILP: cartilage intermediate layer protein; COL1A2: collagen, type 1, alpha 2; COL2A1: collagen, type 2, alpha 1; COMP: cartilage oligomeric matrix protein; COX2: cyclooxygenase-2; DPT: dermatopontin; EASE: Expression Analysis Systematic Explorer; ECM: extracellular matrix; FAP: fibroblast activation protein; GEO: Gene Expression Omnibus; GO: gene ontology; IGF-1: insulin-like growth factor-1; NCBI: National Center for Biotechnology Information; RT-qPCR: quantitative polymerase chain reaction; RPLP0: ribosomal protein, large, P0; SOX9: sex-determining region homeobox-9; TNC: tenascin-C.

Competing interests

The authors declare that they have no competing interests.

Authors' contributions

Experimental surgical procedures were performed by CWM and DDF. Tissue sample harvesting was performed by DDF and MJM. Histological techniques were performed by CWM, DDF, and MJM. Molecular biology studies and bioinformatics analyses were performed by MJM and JNM. Statistical analysis of microarray data was performed by LH, ACB, and AJS. Statistical analysis of RT-qPCR data was performed by MJM. All authors contributed to the writing of this manuscript.

Acknowledgements

Dr. Mark Band and the W.M. Keck Center for Comparative and Functional Genomics at the University of Illinois are graciously acknowledged. The authors also appreciate Rebekah Cosden for her insight into RNA isolation of small samples and Dr. Timothy McClintock for his advice in functional genomics analysis. Financial support was received from the Gluck Equine Research Foundation, The Geoffrey C. Hughes Foundation, The Morris Animal Foundation (Training Fellowship D06EQ-409 to M.M. and the Consortium for Equine Medical Genetics D07EQ-500), and the NIH (KY-INBRE P20 RR16481).

References

1. Riddle WE Jr: **Healing of articular cartilage in the horse.** *Journal of the American Veterinary Medical Association* 1970, **157**:1471-1479.
2. Shapiro F, Koide S, Glimcher MJ: **Cell origin and differentiation in the repair of full-thickness defects of articular cartilage.** *Journal of Bone and Joint Surgery (American)* 1993, **75**:532-553.
3. Mankin HJ: **The reaction of articular cartilage to injury and osteoarthritis.** *The New England Journal of Medicine* 1974, **291**:1285-1292.
4. Vachon AM, McIlwraith CW, Kelley CW: **Biochemical study of repair induced osteochondral defects of the distal portion of the radial carpal bone in horses by use of periosteal autografts.** *American Journal of Veterinary Research* 1991, **52**:328-332.
5. Vachon AM, McIlwraith CW, Trotter GW, Norrdin RW, Powers BE: **Morphologic study of induced osteochondral defects of the distal portion of the radial carpal bone in horses by use of glued periosteal autografts.** *American Journal of Veterinary Research* 1991, **52**:317-327.
6. Frisbie DD, Oxford JT, Southwood L, Trotter GW, Rodkey WG, Steadman JR, Goodnight JL, McIlwraith CW: **Early events in cartilage repair after subchondral bone microfracture.** *Clin Orthop Relat Res* 2003, **407**:215-227.
7. Vachon AM, McIlwraith CW, Powers BE, McFadden PR, Amiel D: **Morphologic and biochemical study of sternal cartilage autografts for resurfacing induced osteochondral defects in horses.** *American Journal of Veterinary Research* 1992, **53**:1038-1047.
8. Rodrigo JJ, Steadman JR, Silliman JF, Fulstone HA: **Improvement of full-thickness chondral defect healing in the human knee after debridement and microfracture using continuous passive motion.** *American Journal of Knee Surgery* 1994, **7**:109-116.
9. Kadiyala S, Young RG, Thiede MA, Bruder SA: **Culture expanded canine mesenchymal stem cell possess osteochondrogenic potential in vivo and in vitro.** *Cell Transplantation* 1997, **6**:125-134.
10. Pittenger MF, Mackay AM, Beck SC, Jaiswal RK, Douglas R, Mosca JD, Moorman MA, Simonetti DW, Craig S, Marshak DR: **Multilineage Potential of Adult Human Mesenchymal Stem Cells.** *Science* 1999, **284**:143-147.
11. Im GI, Kim DY, Shin JH, Hyun CW, Cho WH: **Repair of cartilage defect in the rabbit with cultured mesenchymal stem cells from bone marrow.** *The Journal of Bone & Joint Surgery Br* 2001, **83-B**:289-294.

12. Mithoefer K, Williams RJ III, Warren RF, Potter HG, Spock CR, Jones EC, Wickiewicz TL, Marx RG: **Chondral resurfacing of articular cartilage defects in the knee with the microfracture technique. Surgical technique.** *The Journal of Bone & Joint Surgery* 2006, **88**:294-304.
13. Giovannini S, Brehm W, Mainil-Varlet P, Nesić D: **Multilineage differentiation potential of equine blood-derived fibroblast-like cells.** *Differentiation* 2008, **76**:118-129.
14. Raghunath J, Salacinski HJ, Sales KM, Butler PE, Seifalian AM: **Advancing cartilage tissue engineering: the application of stem cell technology.** *Current Opinion in Biotechnology* 2005, **16**:503-509.
15. Richter W: **Cell-based cartilage repair: illusion or solution for osteoarthritis.** *Current Opinion in Rheumatology* 2007, **19**:451-456.
16. Frisbie DD, Trotter GW, Powers BE, Rodkey WG, Steadman JR, Howard RD, Park RD, McIlwraith CW: **Arthroscopic subchondral bone plate microfracture technique augments healing of large chondral defects in the radial carpal bone and medial femoral condyle of horses.** *Vet Surg* 1999, **28**:242-55.
17. Frisbie DD, Bowman SM, Colhoun HA, DiCarlo EF, Kawcak CE, McIlwraith CW: **Evaluation of autologous chondrocyte transplantation via a collagen membrane in equine articular cartilage defects - results at 12 and 18 months.** *Osteoarthritis and Cartilage* 2008, **16**:667-679.
18. MacLeod JN, Burton-Wurster N, Gu DN, Lust G: **Fibronectin mRNA splice variant in articular cartilage lacks bases encoding the V, III-15, and I-10 proteins segments.** *J Biol Chem* 1996, **271**:18954-18960.
19. MacLeod JN, Fubini SL, Gu DN, Tetreault JW, Todhunter RJ: **Effect of synovitis and corticosteroids on transcription of cartilage matrix proteins.** *American Journal of Veterinary Research* 1998, **59**:1021-1026.
20. Adams ME, Huang DQ, Yao LY, Sandell LJ: **Extraction and isolation of mRNA from adult articular cartilage.** *Anal Biochem* 1992, **202**:89-95.
21. Chomczynski P, Mackey K: **Modification of the TRI Reagent™ procedure for isolation of RNA from polysaccharide- and proteoglycan-rich sources.** *BioTechniques* 1995, **19**:942-945.
22. Eberwine J, Yeh H, Miyashiro K, Cao Y, Nair S, Finnell R, Zettl M, Coleman P: **Analysis of gene expression in single live neurons.** *PNAS USA* 1992, **89**:3010-3014.
23. Feldman AL, Costouros NG, Wang E, Qian M, Marincola FM, Alexander HR, Libutti SK: **Advantages of mRNA amplification for microarray analysis.** *BioTechniques* 2002, **33**:906-914.
24. MacLeod JN: **Equine Articular Cartilage Microarray (abstract).** 2005 [http://www.intl-pag.org/13/abstracts/PAG13_W092.html]. Plant & Animal Genome Conference XII, San Diego, CA, USA
25. Band MR, Olmstead C, Everts RE, Liu ZL, Lewin HA: **A 3800 gene microarray for cattle functional genomics: comparison of gene expression in spleen, placenta, and brain.** *Anim Biotechnol* 2002, **13**:163-172.
26. Rosenzweig BA, Pine PS, Domon OE, Morris SM, Chen JJ, Sistare FD: **Dye-bias correction in dual-labeled cDNA microarray gene expression.** *Environ Health Persp* 2004, **112**:480-487.
27. Scheffé H: *The Analysis of Variance* New York, NY: Wiley; 1959:66.
28. Benjamini Y, Hochberg Y: **Controlling the false discovery rate: a practical and powerful approach to multiple testing.** *J Roy Stat Soc* 1995, **B**:289-300.
29. Altschul SF, Gish W, Miller W, Myers EW, Lipman DJ: **Basic Local Alignment Search Tool.** *J Mol Biol* 1990, **215**:403-410.
30. Coleman SJ, Clinton R, MacLeod JN: **Construction of a master gene list for a 9322 feature equine cDNA microarray (abstract).** 2007 [http://www.intl-pag.org/15/abstracts/PAG15_P050_587.html]. Plant & Animal Genome Conference XV, San Diego, CA, USA
31. Mienaltowski MJ, Huang L, Stromberg AJ, MacLeod JN: **Differential gene expression associated with postnatal equine articular cartilage maturation.** *BMC Musculoskeletal Disorders* 2008, **9**:149.
32. Dennis G Jr, Sherman BT, Hosack DA, Yang J, Gao W, Lane HC, Lempicki RA: **DAVID: Database for Annotation, Visualization, and Integrated Discovery.** *Genome Biology* 2003, **4**:R60.
33. Maglott D, Ostell J, Pruitt KD, Tatusova T: **Entrez Gene: gene-centered information at NCBI.** *Nucleic Acids Research* 2005, **33**:D54-D58.
34. Hosack DA, Dennis G Jr, Sherman BT, Lane HC, Lempicki RA: **Identifying biological themes within lists of genes with EASE.** *Genome Biology* 2003, **4**(10):R70.
35. Vandesompele J, De Preter K, Pattyn F, Poppe B, Van Roy N, De Paepe A, Speleman F: **Accurate normalization of real-time quantitative RT-PCR data by geometric averaging of multiple internal control genes.** *Genome Biology* 2002, **3**:RESEARCH0034.1-0034.11.
36. Ramakers C, Ruijter JM, Lekanne Deprez RH, Moorman AFM: **Assumption-free analysis of quantitative real-time PCR data.** *Neuroscience Letters* 2003, **339**:62-66.
37. Schefe JH, Lehmann KE, Buschmann IR, Unger T, Funke-Kaiser K: **Quantitative real-time RT-PCR data analysis: current concepts and the novel "gene expression's C_T difference" formula.** *Journal of Molecular Medicine* 2006, **84**:901-910.
38. Allanach K, Mengel M, Einecke G, Sis B, Hidalgo LG, Mueller T, Halloran PF: **Comparing microarray versus RT-PCR assessment of renal allograft biopsies: similar performance despite different dynamic ranges.** *Am J Transplantation* 2008, **8**:1006-1015.
39. Burton-Wurster N, Borden C, Lust G, MacLeod JN: **Expression of the (V+C) fibronectin isoform is tightly linked to the presence of a cartilaginous matrix.** *Matrix Biology* 1998, **17**:193-203.
40. Lorenzo P, Bayliss MT, Heinegard D: **A novel cartilage protein (CILP) present in the mid-zone of human articular cartilage increases with age.** *J Biol Chem* 1998, **273**:23463-23468.
41. Salminen H, Perala, Lorenzo P, Saxne T, Heinegard D, Saamanen AM, Vuorio E: **Up-regulation of cartilage oligomeric matrix protein at the onset of articular cartilage degeneration in a transgenic mouse model of osteoarthritis.** *Arth Rheum* 2000, **43**:1742-1748.
42. Giannoni P, Siegrist M, Hunziker EB, Wong M: **The mechanosensitivity of cartilage oligomeric protein (COMP).** *Biorheology* 2003, **40**:101-109.
43. Johnson K, Farley D, Hu S, Terkeltaub R: **One of two chondrocyte-expressed isoforms of cartilage intermediate-layer protein functions as an insulin-like growth factor I antagonist.** *Arth Rheum* 2003, **48**:1302-1314.
44. Koelling S, Clauditz TS, Kaste M, Miosge N: **Cartilage oligomeric matrix protein is involved in human limb development and in the pathogenesis of osteoarthritis.** *Arth Res Ther* 2006, **8**:R56.
45. Murray RC, Smith RK, Henson FMD, Goodship A: **The distribution of cartilage oligomeric matrix protein (COMP) in equine carpal articular cartilage and its variation with exercise and cartilage deterioration.** *Vet J* 2001, **162**:121-128.
46. Piscosa JL, Fermor B, Kraus VB, Stabler TV, Guilak F: **The influence of mechanical compression on the induction of osteoarthritis-related biomarkers in articular cartilage explants.** *Osteoarthritis and Cartilage* 2005, **13**:1092-1099.
47. DiCesare PE, Carlson CS, Stoleran ES, Hauser N, Tulli H, Paulsson M: **Increased degradation and altered tissue distribution of cartilage oligomeric matrix protein in human rheumatoid and osteoarthritic cartilage.** *Journal of Orthopaedic Research* 1996, **14**:946-955.
48. Lafont JE, Talma S, Murphy CL: **Hypoxia-inducible factor 2α is essential for hypoxic induction of the human articular chondrocyte phenotype.** *Arth Rheum* 2007, **56**:3297-3306.
49. Mackie EJ, Tucker RP: **The tenascin-C knockout mouse revisited.** *Journal of Cell Science* 1999, **112**:3847-3853.
50. Chiquet-Ehrismann R, Tucker RP: **Connective tissues: signaling by tenascins.** *The International Journal of Biochemistry & Cell Biology* 2004, **36**:1085-1089.
51. Hsai HC, Schwarzbauer JE: **Meet the tenascins: multifunctional and mysterious.** *The Journal of Biochemistry* 2005, **250**:26641-26644.
52. Metzger M, Bartsch S, Bartsch U, Bock J, Schachner M, Braun K: **Regional and cellular distribution of the extracellular matrix protein tenascin-C in the chick forebrain and its role in neonatal learning.** *Neuroscience* 2006, **141**:1709-1719.
53. Mackie EJ, Ramsey S: **Expression of Tenascin in joint-associated tissues during development and postnatal growth.** *Journal of Anatomy* 1996, **188**:157-165.
54. Mackie EJ, Murphy LI: **The role of Tenascin-C and related glycoproteins in early chondrogenesis.** *Microscopy Research and Technique* 1998, **43**:102-110.
55. Pfander D, Heinz N, Rothe P, Carl H-D, Swoboda B: **Tenascin and aggrecan expression by articular chondrocytes is influenced by interleukin 1β: a possible explanation for the changes in matrix synthesis during osteoarthritis.** *Ann Rheum Dis* 2004, **63**:240-244.

56. Garin-Chesa P, Old LJ, Rettig WJ: **Cell surface glycoprotein of reactive stromal fibroblasts as a potential antibody target in human epithelial cancers.** *PNAS USA* 1990, **87**:7235-7239.
57. Milner JM, Kevorkian L, Young DA, Jones D, Wait R, Donell ST, Barksby E, Patterson AM, Middleton J, Cravatt BF, Clark IM, Rowan AD, Cawston TE: **Fibroblast activation protein alpha is expressed by chondrocytes following a pro-inflammatory stimulus and is elevated in osteoarthritis.** *Arthritis Research & Therapy* 2006, **8**(1):R23.
58. Forbes EG, Cronshaw AD, MacBeath JR, Hulmes DJ: **Tyrosine-rich acidic matrix protein (TRAMP) is a tyrosine-sulphated and widely distributed protein of the extracellular matrix.** *FEBS Letters* 1994, **351**:433-436.
59. Okamoto O, Fujiwara S: **Dermatopontin, a novel player in the biology of the extracellular matrix.** *Connective Tissue Research* 2006, **47**:177-189.
60. Tallheden T, Karlsson C, Brunner A, Lee J Van Der, Hagg R, Tommasini R, Lindahl A: **Gene expression during redifferentiation of human articular chondrocytes.** *Osteoarthritis and Cartilage* 2004, **12**:525-535.
61. Arasapam G, Scherer M, Cool JC, Foster BK, Xian CJ: **Roles of COX-2 and iNOS in the bony repair of the injured growth plate cartilage.** *Journal of Cellular Biochemistry* 2006, **99**:450-461.
62. Wolff DA, Stavenson S, Goldberg VM: **S-100 protein immunostaining identifies cells expressing a chondrocytic phenotype during articular cartilage repair.** *Journal of Orthopaedic Research* 1992, **10**:49-57.
63. Brew CJ, Clegg PD, Boot-Handford RP, Andrews G, Hardingham T: **Gene expression in human chondrocytes in late OA is changed in both fibrillated and intact cartilage without evidence of generalised chondrocytes hypertrophy.** *Ann Rheum Dis* 2009, **0**: ar.d.2008.097139v1[epub]

Pre-publication history

The pre-publication history for this paper can be accessed here:

<http://www.biomedcentral.com/1755-8794/2/60/prepub>

Publish with **BioMed Central** and every scientist can read your work free of charge

"BioMed Central will be the most significant development for disseminating the results of biomedical research in our lifetime."

Sir Paul Nurse, Cancer Research UK

Your research papers will be:

- available free of charge to the entire biomedical community
- peer reviewed and published immediately upon acceptance
- cited in PubMed and archived on PubMed Central
- yours — you keep the copyright

Submit your manuscript here:
http://www.biomedcentral.com/info/publishing_adv.asp

